Journal of Biosensors & Bioelectronics
ISSN: 2155-6210

Ducote et al., J Biosens Bioelectron 2016, 7:4
DOI: 10.4172/2155-6210.1000224

Research Article Open Access

Electrochemical Impedance Spectroscopy (EIS) as a Tool for Pathogen Detection

Ducote M[1], Vinson BT[2], Hogquist S[3], Riggs B[1], Saksena J[3] and Chrisey DB[1,3]*

[1]Department of Physics and Engineering-Physics, Tulane University, New Orleans, LA, USA
[2]Bioinnovation Program, Tulane University, New Orleans, LA, USA
[3]Department of Biomedical Engineering, Tulane University, New Orleans, LA, USA

Abstract

Background: In the event of a biological warfare attack, prompt real-time detection methods are necessary to identify the presence of a pathogen well before victims begin exhibiting symptoms in order to allow sufficient time for therapeutic intervention. Current techniques for detecting the presence of biological warfare agents in high-risk environments are exclusively structure-based, relying on the identification of key structural components of specific pathogens that are already well-known and studied. These techniques provide no defense against the modern capability to synthesize new and unfamiliar pathogens of an arbitrary structure that could evade these detection mechanisms.

Methods/Results: This investigation tested the prospect of using electrochemical impedance spectroscopy (EIS) to create a real-time function-based biosensor to identify any cytotoxic substance, whether known or unknown, without regard to its structure. The concept was tested by exposing A549 epithelial adenocarcinoma cells to ricin in several concentrations, ranging from 1 ng/mL to 1000 ng/mL, and observing the effect on the measured impedance of the cells. With as few as three unique trials for each concentration, a statistically significant difference was observed between the impedance data for ricin-exposed cells and that of a ricin-free control group. By comparing the change in the impedance of each sample over periods of 60 minutes and 4 hours, statistically significant detection was achieved within timeframes ranging from 65 minutes after adding 1000 ng/mL ricin to 45 hours after adding 1 ng/mL ricin.

Conclusion: EIS provides a highly sensitive, real-time, and non-destructive method to identify the presence of a cytotoxin. EIS demonstrates rapid detection times that become faster as the concentration increases. Further analysis describes how the design of a potential biosensing device could be used to convert an arbitrary airborne concentration to a media concentration sufficiently large as to achieve detection within the window of time necessary for therapeutic intervention.

Keywords: Electrical impedance spectroscopy; ECIS; Pathogen sensing; Biological warfare; Airborne pathogens

Introduction

The technique of electrochemical impedance spectroscopy (EIS) measures the impedance of an object of interest in real time to monitor changes in its properties or behavior. For this biosensing application, the goal is to use this technique to study the response of cells exposed to a known toxin in real time by continually measuring the impedance between two electrodes separated by a confluent cell monolayer in electrolytic media. In the interest of using an accepted standard to extract initial proof-of-concept data for this application, this investigation employed commercially produced technology, Electric Cell-substrate Impedance Sensing (ECIS). This system, which was devised in 1991 by Don Giaever and Charles Keese [1], has achieved widespread use in subsequent years because it yields real-time data as the cells grow and interact with their environment [2-4]. Moreover, this technique does not require labels or other chemical treatments conventionally employed to measure cellular endpoints and which can potentially affect the behavior of the cells.

Raw data of impedance as a function of frequency and time may be used at a simplistic level to observe responses to the addition of a stimulus or differences in the trend lines between different treatments or cell types. However, the creators of the ECIS system also derived a detailed equivalent circuit model [1] for the cell layer that allows the data obtained for resistance and capacitance to be interpreted in terms of parameters corresponding to different components of the cell structure. This model is founded on the assumption that as the cell monolayer forms and covers the electrodes, the cells act as insulators that separate the current from the electrolytic media in which they are cultured. This results in an increase in the impedance in response to the growth of new cells. The path of the current as it passes from the electrodes through the cell layer is assumed [1] to be as shown in Figure 1.

Use of ECIS has become widespread in biology laboratories due to its usefulness in monitoring the growth, confluence, substrate adherence, micromotion, morphology, and death of cultured cells over time [5-9]. This paper seeks to expand these capabilities outside of the laboratory in order to lay the foundation for development of a real-time, function-based biosensor. Such a biosensor could be utilized as a preventative measure against biological warfare through the detection of bacteria, viruses, spores and/or other toxins that may be introduced into the environment (typically via airborne vehicles).

***Corresponding author:** Douglas B Chrisey, Department of Physics and Engineering-Physics, Tulane University, New Orleans, LA, Tel: 5048655090; E-mail: douglasbchrisey@gmail.com

Received October 13, 2016; **Accepted** October 18, 2016; **Published** October 28, 2016

Citation: Ducote M, Vinson BT, Hogquist S, Riggs B, Saksena J, et al. (2016) Electrochemical Impedance Spectroscopy (EIS) as a Tool for Pathogen Detection. J Biosens Bioelectron 7: 224. doi: 10.4172/2155-6210.1000224

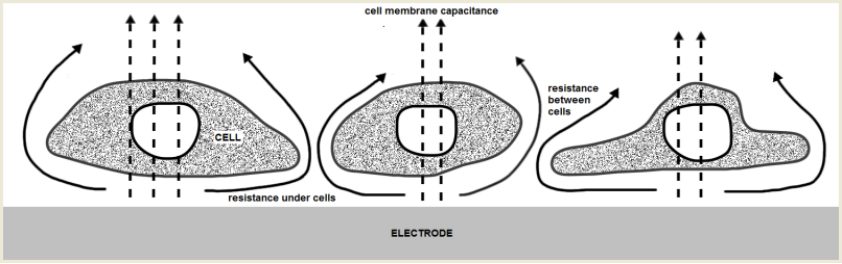

Figure 1: Diagram of current flow passing from the electrode through the cell layer. Solid lines indicate the path taken by current at low frequencies; dotted lines indicated the current path at high frequencies.

Existing methods to counter such tactics work to identify pathogens by their structure, and are developed by examining the structural features of known biological warfare agents and creating a sensor that detects certain key identifying features [10,11]. The crucial weakness of this technology is that it can only examine the structural attributes of already known pathogens, rendering it helpless against any structures that may be unfamiliar to the designers of the sensor. The capabilities of genetic engineering make this technology easy to exploit by allowing the creation of synthetic pathogens with original structures, guaranteeing that they will be unrecognizable to any structure-based sensors [12]. Thus, development of an EIS functional biosensing system holds value as it would be able to detect the presence of any pathogen based on its interaction with mammalian cells, rather than based on some component of its structure. Here we present a novel system that is capable of detecting anomalies in the behavior of a confluent cell layer as a whole, intercellular junctions, and even internal organelles; thus giving it the potential to identify any pathogen by virtue of it being pathogenic rather than its resemblance to previously encountered biological weapons.

To test the efficacy of such a system, ricin was chosen as an example pathogen due to its frequent use as a biological warfare agent as well as its relatively low potency (and therefore low detectability) compared to other common choices for biological weapons [13]. Ricin is a polypeptide that catalyzes the hydrolysis of an adenine residue from the 28S subunit of ribosomal RNA, inactivating the ribosome. Ricin has the ability to rapidly inactivate extraordinary numbers of ribosomes within a cell, thus preventing the cell from producing proteins and ultimately causing cell death [14-16]. Although ricin is significantly less toxic than many weaponizable pathogens such as anthrax and botulinum, it is often used because of its low cost and ease of accessibility relative to these and other alternatives [17]. That this toxin is among the most likely to fall into the hands of an attacker, coupled with its lower toxicity enabling it to test the lower limits of the system's sensitivity, makes it an ideal choice to study the prospects of an EIS-based pathogen sensor.

Materials and Methods

Cell line

Human alveolar basal epithelial adenocarcinoma cells (A549) were cultured in Dulbecco's Modified Eagle Medium (DMEM) supplemented with 10% Fetal Bovine Serum (FBS), 1% essential amino acids, 1% non-essential amino acids, 1% sodium pyruvate, and 1% anti/anti. Lung cells were chosen as the most representative because they are the ones directly exposed to any airborne substances during inhalation [18]. All media and supplements were obtained from Life Technologies (Carlsbad, CA), unless otherwise stated.

Toxin

Ricin toxin, isolated from Ricinus communis seeds, was obtained from BEI Resources (Manassas, VA). The toxin was diluted to four concentrations in phosphate buffered saline (PBS) prior to cell treatment. Cells were exposed to final concentrations of 1 ng/mL, 10 ng/mL, 100 ng/mL, and 1000 ng/mL. Each concentration of ricin was applied to 3 of the 15 cell-containing wells, while the remaining 3 continued to contain the original ricin-free media + vehicle (PBS).

Impedance measurements

Cells were seeded on two, 8-well plates (8W10E+; Applied Biophysics, Troy, NY) at a concentration of 1.0 × 105 cells/mL. The plates consist of 8 wells each containing 40, 250 µm interdigitated gold electrodes. Two plates were connected simultaneously to the ECIS instrument to conduct measurements of a total of 16 wells, each containing 400 µL of culture media. A single well containing media but no cells served as a control. The cells were cultured in an incubator at 37 °C and 5% CO_2. After 20 hours, the culture media was changed and ricin was added to the appropriate wells. Measurement then continued for an additional 72 hours. The ECIS Zθ instrument used to conduct impedance measurements consists of a lock-in amplifier in parallel with a 1V AC signal and a 1 MΩ resistor. During each measurement, the frequency of the alternating current varies in multiples of two within the range of 62.5 Hz to 64 kHz. The impedance, resistance, and capacitance are measured at each of the 11 frequencies. The device continually cycles through taking measurements of each well, with an approximate interval of 4 minutes between 2 consecutive measurements of a single well. Measurements were paused while cells were removed from the incubator during media changes.

Analysis

Data for all cell-containing wells were normalized by substracting the impedance and resistance of the media-only control to remove circuit components of the media and electrodes and obtain the impedance and resistance of the cell monolayer alone. For capacitance, the normalized value for each cell-containing well was calculated by removing the media-only capacitance as if it were in series with the normalized capacitance, i.e., according to the expression Cn = (Cr-1 – Cm-1)-1, where Cn is the normalized capacitance, Cr is the raw data capacitance, and Cm is the media capacitance. To determine the optimal frequency for observing each of the three measurement parameters, the signal-to-noise ratio for each frequency was calculated at each of the fifteen cell-containing wells at time 24 hours. The signal-to-noise ratio of each measurement parameter was calculated as the ratio of the normalized value of the parameter to the value of the same parameter in the media control. This ratio was averaged over all 15

cell-containing wells to determine the mean signal strength for each frequency, and the frequency exhibiting the highest signal strength was chosen to observe impedance, resistance, and capacitance.

Results

The mean signal strength of the impedance, resistance, and capacitance data was tabulated for each of the surveyed frequencies and was found to reach its maximum value at 16 kHz, 4 kHz, and 64 kHz for impedance, resistance, and capacitance, respectively. The trend of the signal-to-noise ratio for each of the 3 measured parameters is plotted in Figure 2. Since these minimum-noise frequencies provide the clearest representation of the data, these were the frequencies used for observation of the behavior of the three measured parameters over time.

To account for possible impedance contributions from the equipment setup, all data were normalized by subtracting the measured values for the media control from those of all other wells. The data were further normalized to account for the effects of any differences in the initial impedance between the wells by expressing the normalized value as a multiple of the value for that well immediately before adding the toxin. The normalized impedance at 16000 Hz is shown in Figure 3. The graph includes representative data from one trial for each of the five treatments, ranging from no ricin to a ricin concentration of 1000 ng/mL.

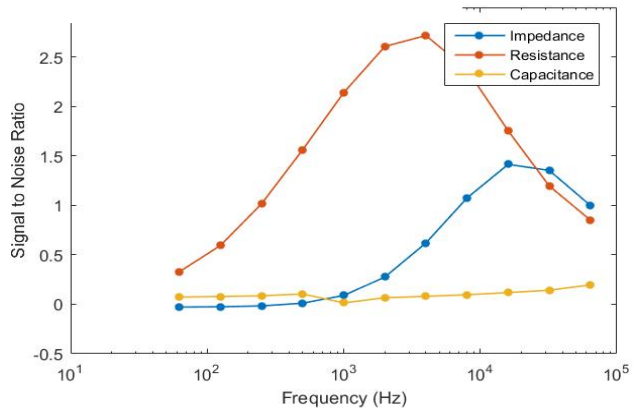

Figure 2: Average signal to noise ratio (24 hours). Signal strength of the impedance, resistance, and capacitance data at each of the eleven frequencies surveyed by ECIS. The maximum signal strength is exhibited at 16 kHz for impedance data, 4 kHz for resistance data, and 64 kHz for capacitance data.

In the case of the cells not exposed to ricin, the impedance at first increased at a steady pace but began to slow around 40 hours and eventually leveled off. Those exposed to 10, 100, and 1000 ng/mL at first experienced a steep spike in impedance, which did not occur as quickly for the 10 ng/mL treatments as for the higher concentrations. However, this increase was only temporary, and the impedance peaked 7 hours after the addition of ricin for the 100 and 1000 ng/mL treatments and 12 hours after the addition of ricin for the 10 ng/mL treatment. The impedance then began declining to ultimately approach a normalized impedance of 0, meaning the impedance approached the value that it takes when no cells were present on the electrode. For the 1 ng/mL treatment, the impedance at first appeared to behave the same as that for which no ricin was added, indicating that the presence of the ricin went undetected. Notwithstanding, around 21 hours after the addition of ricin it too began to diverge from the trend line of the unexposed cells. The impedance ultimately began to steadily decline even for this treatment level. The presence of the ricin was therefore clearly detectable at all four concentrations; detection is merely delayed at lower concentrations.

The impedance differences between groups at any discrete time point were not as pronounced as differences in the impedance change over time. Thus, the change in impedance over a fixed length of time was used for a statistical comparison of the groups. Six time intervals between 4 minutes and 4 hours were analyzed to determine statistical significance. 60 minutes was found to be the shortest time interval over which differences in the impedance change were statistically significant between any of the treatment groups. Consequently, as the first metric of the impedance change, the difference between the impedance at each point in time and the impedance 60 minutes earlier was calculated for each concentration group. The average of the 3 trials for each group is plotted in Figure 4. Although the 60-minute change data for the 1 ng/mL ricin treatment group was similar to that for the control group for the duration of the experiment, the other three treatment groups nearly immediately exhibited much larger 60-minute changes than did the control group.

The 2-sample t-test was used to compare each of the 4 ricin groups to the control group and determine when a statistically significant detection could be made. 95% statistical significance was chosen as the threshold for acceptance, allowing a 5% probability of false positives.

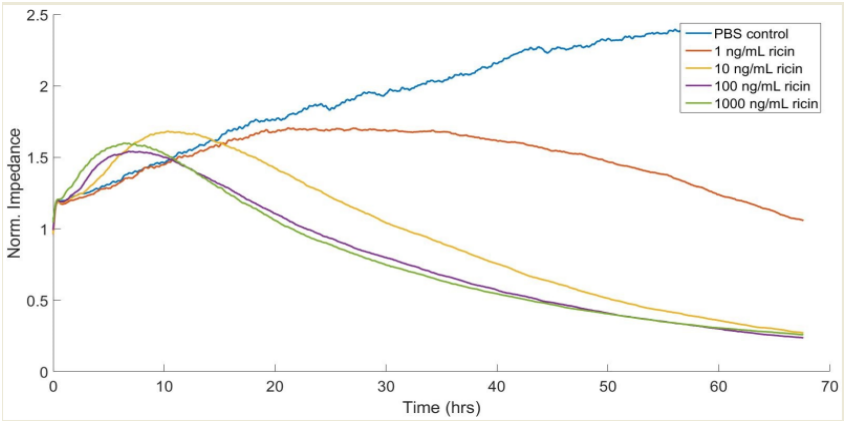

Figure 3: Normalized impedance over time at 16000 Hz. Toxin was added at t=0.

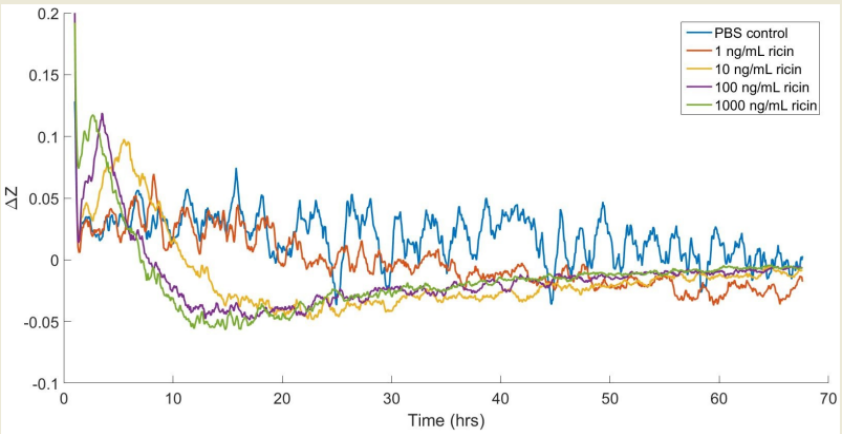

Figure 4: 60-minute impedance change, 16000 Hz. The difference between the normalized impedance at each point in time and the normalized impedance 60 minutes earlier, for data taken at 16000 Hz. For ricin concentrations 10-1000 ng/mL, the impedance change was initially much larger than for the control group; for ricin concentration of 1 ng/mL, the impedance change failed to ever appear consistently different from the control group.

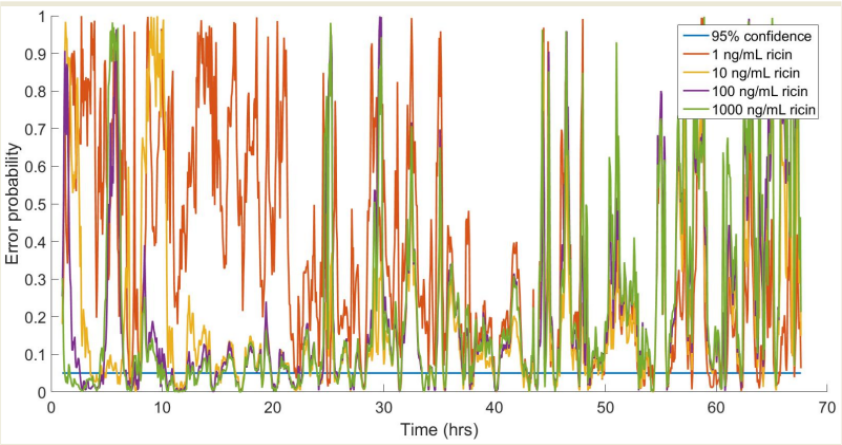

Figure 5: 2-sample t-test results, 60-minute impedance change. Results of the two-sample t-test comparing the 60-minute impedance change group to the control group. Detection was achieved with 95% confidence after 65 minutes for the 1000 ng/mL ricin sample, 109 minutes for the 100 ng/ml sample, and 157 minutes for the 10 ng/mL sample. 95% detection probability was never consistently achieved for the 1 ng/mL sample.

The probability of making a false detection is shown as a function of time for each experimental group in Figure 5. While the 10, 100, and 1000 ng/mL treatment groups achieve the detection criteria within hours, the t-test results for the 1 ng/mL group drift erratically for the entirety of the measurement period, occasionally slipping into the 95% confidence range. Because of the allowed 5% (1 in 20) probability of error, about once every 20 hours even statistically indistinguishable groups erroneously register statistically significant deviation. To preclude the possibility of false detections due to statistical noise, we introduce the criterion of "consistency" as a means of checking the validity of a detection if several hours have elapsed before it occurs. We say that a sample "consistently" exhibits 95% confidence if it does so for a period of at least 60 minutes, meaning that the test signaled detection for 2 consecutive non-overlapping 60-minute intervals. For tests conducted using shorter or longer time intervals, the criterion for consistent detection is adjusted correspondingly.

An interval as small as 60 minutes is necessary to avoid a large time delay in acquiring impedance change data so that we can obtain rapid detection for the quickly-responsive higher concentrations. However, due to the slow response at a concentration of 1 ng/mL, steep changes were never observed within a 60-minute window, thus preventing this group from ever remaining consistently below a 5% probability of false positives using this method. After analyzing the impedance change over several longer time intervals, we observed that the smallest time interval to consistently exhibit 95% confidence was 4 hours. We therefore used a second method of calculating the difference in impedance at each point in time and the time 4 hours earlier. The average of the 4-hour impedance changes for each experimental group is displayed in Figure 6. The 10-1000 ng/mL groups again saw an immediate sharp deviation from the control group, but with this metric we are delayed in observing this deviation until after four hours have elapsed. However, a much clearer contrast can now be seen between the 1 ng/mL ricin group and the ricin-free control group.

The 2-sample t-test was conducted again using the new metric, with 95% statistical significance again being used as the threshold for determining detection. The probability of an erroneous detection using this method is shown as a function of time for each group in Figure 7. While the detection time for concentrations of 10 ng/mL or larger is rendered useless due to the 4-hour time delay, this method is useful in granting consistent statistically significant detection for the 1 ng/mL group after 45 hours. As the 60 minute impedance change is optimal for concentrations of 10 ng/mL or larger and the 4-hour

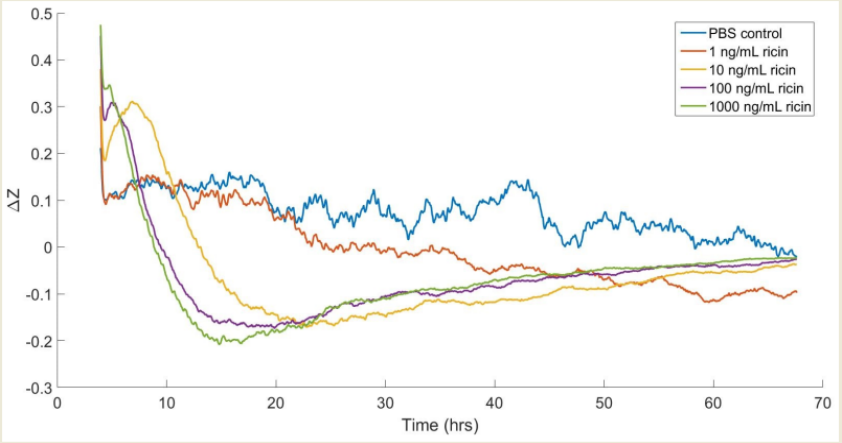

Figure 6: 4-hour impedance change, 16000 Hz. The difference between the normalized impedance at each point in time and the normalized impedance four hours earlier, for data taken at 16000 Hz. For ricin concentrations 10-1000 ng/mL, the impedance change was initially much larger than for the control group; for ricin concentration of 1 ng/mL, more than 30 hours elapsed before there was any noticeable difference from the control group.

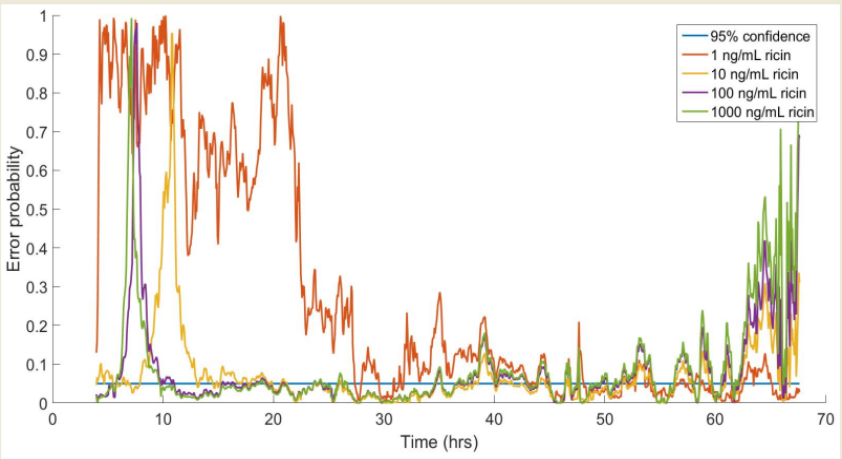

Figure 7: 2-sample t-test results, 4-hour impedance change: Results of the 2-sample t-test comparing the four-hour impedance change group to the control group. 95% detection probability was consistently achieved after 45 hours for the 1 ng/mL ricin sample. Due to the necessary 4-hour wait time before one can even begin calculating this metric, detection for all other samples was already achieved beforehand using the sixty-minute impedance change.

impedance change is optimal for concentrations of 1 ng/mL or smaller, the combination of the 2 methods yields a robust tool for identifying ricin at the entire range of concentrations within the duration of the experiment.

Discussion

The steady increase in impedance observed for the vehicle control group is similar to the typical impedance behavior for various cell lines in DMEM-based media [19-21], which is widely understood to indicate an increase in electrode coverage due to continued cell growth [1,5,6,22]. The vehicle alone, therefore, had no observable effect on the health and ordinary growth patterns of the cells. The early impedance response of the 1 ng/mL experimental group likewise resembled behavior indicative of normal cell growth [4-7,9], suggesting that the toxin did not immediately result in a decrease in cell viability. However, the ultimate drop in impedance for this group shows that cell monolayer breakdown did eventually occur, presumably due to the cell death that is the ultimate consequence of ricin exposure [14-16]. Because ricin begins to inhibit protein synthesis within a timeframe several orders of magnitude shorter than it displays any signs of cytotoxicity [23,24], it is likely that ricin began to induce ultimately fatal changes to internal cell behavior long before they could be detected for this concentration group. Further research could confirm this by changing the cells to ricin-free media after a limited exposure period and verifying that monolayer dissolution still eventually occurs after a lengthy delay.

All cell cultures exposed to ricin concentrations of 10 ng/mL or larger similarly showed significant negative trends in the impedance data after an initial period of upward movement, with the progressively earlier onset of the impedance decrease at higher concentrations suggesting that cell death occurs quicker when the quantity of ricin is larger. The difference between the critical points of concentration groups was most pronounced between the 1 and 10 ng/mL groups (a reduction from 22 hours to 11 hours) and between the 10 and 100 ng/mL groups (a reduction from 11 hours to 7 hours). Conversely, the difference between the rate of the impedance response of the 100 and 1000 ng/mL treatments was statistically insignificant, implying that the ricin may reach a maximum cell response at some concentration between 10

and 100 ng/mL. This may be clarified by further experimentation with larger sample sizes or with various other concentrations spanning the range from 10 to 1000 ng/mL.

More interesting than the later-occurring distinction between groups based on their impedance drops, however, is the much faster and larger initial increase in impedance of the groups with 10 ng/mL+ ricin compared to vehicle and low toxin concentration (1 ng/mL) groups. This is a counterintuitive occurrence because the ultimate effect of ricin is to destroy cell monolayers [25], not increase the strength of their coverage. Since ricin ultimately causes cell death by disassembling crucial nucleotides in ribosomal RNA and thus preventing protein synthesis [14-16], this decrease in monolayer permeability is possibly a more immediate consequence of the lack of protein production. The specific nature of this effect is an interesting phenomenon which warrants further study. Whatever the mechanism, this aspect of the impedance data is responsible for the most crucial insight that the impedance spectroscopy system yields, identifying the presence of the toxin immediately as it becomes active within cells rather than once it induces cell death.

Implementation

Based on the results of this statistical analysis, the elapsed time before detection can occur may be reliably predicted as a function of media concentration. However, the question remains whether this time interval can be made sufficiently small to allow for effective therapeutic intervention. The standard for making such a determination relies on the LD50, or the median lethal dosage of ricin or any other toxin in a human population [26,27]. This lethal dose is expressed as a mass fraction of toxin quantity compared to the average human body weight, and for ricin this value has been estimated to be 5-10 μg/kg [28]. Given that humans typically inhale air at a rate of about 7 liters per minute [29], the amount of time that elapses before accumulating the lethal dose may be determined based on the mass fraction of airborne ricin. The goal in constructing the system design for a pathogen sensing device is to produce a certain toxin concentration in media in proportion to the airborne concentration in the external environment such that the resulting detection time for that media concentration is an order of magnitude smaller than the time to accumulate a lethal dose at that airborne concentration.

Given an operational setup where air is bubbled through a supply of media to produce the media sample to be exposed to the cells, this situation could be modeled using the diffusion equation to determine the toxin concentration in the media supply at a given time as a function of the original concentration of media. The diffusion coefficient for ricin in media has been experimentally observed to be within the range of 1-2 × 10-10 cm^2/sec [30]. Given a vessel with one face exposed to air containing an unknown concentration of some toxin, the concentration of the toxin at any other point in the vessel may be modeled using the one-dimensional diffusion equation. The shape and layout of the vessel as well as the location of the air opening may be varied, as may be the time for which this process is allowed to occur in order to magnify the concentration of the toxin in the media to the desired multiple of the aerial concentration. This method may be used to obtain any arbitrary concentration of a toxin in the media exposed to cells in order to obtain an appropriately quick response time. Future work should focus on creating the specific design for such a device to create the ideal relationship between system detection time and biological response time.

Conclusion

Studies with the EIS system consistently demonstrated the ability to detect the toxin ricin within a timeframe that decreases with concentration to become as short as 60 minutes, which in most cases is sufficient to evacuate exposed persons and apply treatment [31,32]. In cases where a swifter detection time is necessary, the concentration of toxin in media may be increased to an arbitrarily large multiple of that in the external environment by simply varying parameters of the design of the system used to generate a media supply from the external air. Samples not exposed to any toxin consistently demonstrated behavior completely distinct from exposed samples, resulting in the complete absence of false positive detections with the EIS system. All of this was completed without reliance on information about the structure of the exposed toxin; the ricin was discovered merely by its effect on exposed cells thus making the system successful as a truly real-time function-based biosensor.

Future research could strengthen the viability of this technique by confirming its effectiveness on other toxins distinct from ricin both in structure and mechanism of action. Other experiments could attempt to expand its effectiveness by measuring the behavior of other cell types. Additional research can employ this same technique using a high-frequency impedance analyzer rather than ECIS, enabling capacitive interactions with intracellular components that act as insulators at low frequencies. This work will facilitate the development of a more advanced equivalent circuit model than that used for ECIS, thus refining the statistical model used to estimate the time response and further ensure that a predictably speedy detection can be achieved at any input concentration.

Acknowledgments

This work was made possible in part by the Tulane University School of Science and Engineering Start Up funding.

References

1. Giaever I, Keese C (1991) Micromotion of mammalian cells measured electrically. Proceedings of the National Academy of Sciences 88: 7896-7900.
2. Wegener J, Keese C, Giaever I (2000) Electric Cell-Substrate Impedance Sensing (ECIS) as a noninvasive means to monitor the kinetics of cell spreading to artificial surfaces. Exp Cell Res 259: 158-166.
3. Keese C, Bhawe K, Wegener J, Giaever I (2002) Real-time impedance assay to follow the invasive activities of metastatic cells in culture. BioTechniques 33: 842-850.
4. Stolwijk J, Hartmann C, Balani P, Albermann S, Keese C, et al. (2011) Impedance analysis of adherent cells after in situ electroporation: non-invasive monitoring during intracellular manipulations. Biosens Bioelectron 26: 4720-4727.
5. Giaever I, Keese C (1993) A morphological biosensor for mammalian cells. Nature 366: 591-592.
6. Keese C, Giaever I (1994) A biosensor that monitors cell morphology with electrical fields. IEEE Eng Med Biol Mag 13: 402-408.
7. Keese C, Karra N, Dillon B, Goldberg A, Giaever I (1998) Cell-substratum interactions as a predictor of cytotoxicity. In Vitr Mol Toxicol 11: 183-192.
8. Luong J, Habibi-Razaei M, Meghrous J, Xiao C, Male K, et al. (2001) Monitoring motility, spreading, and mortality of adherent insect cells using an impedance sensor. Anal Chem 73: 1844-1848.
9. Xiao C, Lachance B, Sunahara G, Luong J (2002) An in-depth analysis of electric cell-substrate impedance sensing to study the attachment and spreading of mammalian cells. Anal Chem 74: 1333-1339.
10. Rider T, Petrovick M, Nargi F, Harper K, Schwoeber E, et al. (2003) A B cell-based sensor for rapid identification of pathogens. Science 301: 213-215.
11. Skottrup P, Nicolaisen M, Justesen A (2008) Towards on-site pathogen detection using antibody-based sensors. Biosens Bioelectron 24: 339-348.

12. Fraser C, Dando M (2001) Genomics and future biological weapons: the need for preventive action by the biomedical community. Nature Genet 29: 253-256.

13. Kortepeter M, Parker G (1999) Potential biological weapons threats. Emerg Infect Diseases 5: 523-527.

14. Lord J, Roberts L, Robertus J (1994) Ricin: structure, mode of actions, and some current applications. The FASEB Journal 8: 201-208.

15. Wellner R, Hewetson K, Poli M (1995) Ricin: mechanism of action, detection, and intoxication. J Toxicol 14: 483-522.

16. Doan L (2003) Ricin: mechanisms of toxicity, clinical manifestations, and vaccine development. A review. J Toxicol Clin Toxicol 42: 201-208.

17. Schep L, Temple W, Butt G, Beasley M (2009) Ricin as a weapon of mass terror – separating fact from fiction. Environ Int 35: 1267-1271.

18. Heijink I, Brandenburg S, Noordheuk J, Postma D, Slebos D, et al. (2010) Characterization of cell adhesion in airway epithelial cell types using electric cell-substrate impedance sensing. Eur Respir J 35: 894-903.

19. Müller J, Thirion C, Pfaffl M (2011) Electric cell-substrate impedance sensing (ECIS) based real-time measurement of titer dependent cytotoxicity induced by adenoviral vectors in an IRI-2I cell culture model. Biosens Bioelectron 26: 2000-2005.

20. Jiang A, Zhao H, Cai J, Jiang W (2016) Possible effect of muscle-relaxant anaesthetics on invasion, adhesion, and migration of breast cancer cells. Anticancer Res 36: 1259-1265.

21. Mondal D, Roy CC (2013) Extended electrical model for impedance characterization of cultured HeLa cells in non-confluent state using ECIS electrodes. IEEE Trans Nanobioscience 12: 239-246.

22. Keese C, Giaever K (1990) A whole cell biosensor based on cell-substrate interactions. Proceedings of the Twelfth Annual International Conference of the IEEE.

23. Sidell F, Takafuji E, Franz D (1997) Medical aspects of chemical and biological warfare. Borden Institute, Washington, DC.

24. Lord M, Jolliffe N, Marsden C, Pateman C, Smith D, et al. (2003) Ricin: mechanisms of cytotoxicity. Toxicological Reviews 22: 53-64.

25. Lindstrom A, Erlandsen S, Kersey J, Pennell C (1997) An in vitro model for toxin-mediated vascular leak syndrome: ricin toxin A chain increases the permeability of human endothelial cell monolayers. Blood 90: 2323-2334.

26. Zbinden G, Flury-Roversi M (1981) Significance of the LD_{50}-test for the toxicological evaluation of chemical substances. Archives of Toxicology 47: 77-99.

27. Randhawa M (2009) Calculation of LD_{50} values from the method of Miller and Tainter, 1944. Journal of Ayub Medical College 21: 184-185.

28. Bradberry S, Dickers K, Rice P, Griffiths G, Vale J (2003) Ricin poisoning. Toxicology Review 22: 65-70.

29. Lordo B, Sanford J, Mohnson M (2006) Revision of the metabolically-derived ventilation rates within the exposure factors handbook. Battelle Institute, Columbus, Ohio.

30. Bellelli A, Ippoliti R, Brunori M, Kam Z, Benveniste M, et al. (1990) Binding and internalization of ricin labelled with fluorescein isothiocyanate. Biochem Biophys Res Commun 169: 602-609.

31. Cook D, David J, Griffiths G (2006) Retrospective identification of ricin in animal tissues following administration by pulmonary and oral routes. Toxicology 223: 61-70.

32. Griffiths G, Lindsay C, Allenby A, Bailey S, Scawin J, et al. (1995) Protection against inhalation toxicity of ricin and abrin by immunization. Human and Experimental Toxicology 14: 155-164.